

NILU: TR 10/2003
REFERENCE: E-102155
DATE: OCTOBER 2003
ISBN: 82-425-1505-0

Three-dimensional wind field estimates in complex terrain

George Mocioaca and Bjarne Sivertsen

Contents

	Page
Contents	1
Summary	2
1 Introduction	3
2 Model descriptions	3
2.1 MATHEW	3
2.2 TAPM 3	
3 The test area and the database	4
3.1 Topographical features	4
3.2 The measurement network and database.....	5
3.3 Site representativity evaluation	6
4 Wind field modelled with MATHEW	7
4.1 Results and comparison with observed data	8
4.1.1 Valley sites	8
4.1.2 Ridge sites	9
4.1.3 Open plain sites	10
4.2 Wind speeds modelled with MATHEW	11
5 Wind field modelled with TAPM	12
5.1 Results and comparison with observed data	13
5.1.1 Valley sites	13
5.1.2 Elevated sites	13
5.1.3 Open plain sites	14
5.1.4 TAPM characteristics	15
5.2 Wind speeds modelled with TAPM	16
6 Comparisons of the wind field with MATHEW and TAPM	17
6.1.1 Wind fields	17
6.1.2 Wind speed profiles.....	20
6.1.3 Wind direction profiles.....	21
7 Conclusions	22
8 References	23

Summary

Air pollution dispersion modelling in complex terrain is dependent upon adequate modelling of the three dimensional wind fields. Several wind field models have been developed and tested. This paper presents the results of the application of two different wind field models, which have been applied for simulating the winds in a complex terrain area with coastlines, valleys and mountains.

Local circulations and mesoscale effects due to topographical features as well as land sea breezes modify the wind field to give inhomogeneous and instationary conditions. Numerical dispersion models will need these characteristics as input to enable the estimate of concentrations in an area of this kind.

For simulation of winds in this investigation we have applied one diagnostic and one prognostic wind field model. These models are currently being used on a local and up to mesoscale dispersion estimates at Norwegian Institute for Air Research (NILU).

The diagnostic wind field model, MATHEW, is based on interpolation of wind observations or assimilated data from mesoscale models. It is currently applied for providing wind field input for NILU developed the dispersion model EPISODE. MATHEW is a modified version of the MATHEW model developed by Sherman.

The second wind field model is incorporated in the meteorological component of the air pollution model (TAPM) developed at CSIRO in Australia (Hurley, 2002). TAPM includes a prognostic numerical model that solves the equations for momentum for the horizontal wind components, the incompressible continuity equation for vertical velocity, and scalar equations for potential virtual temperature and specific humidity of water vapour, cloud water and rainwater. The wind field model of TAPM has been used as a "stand alone" model for the purpose of estimating the wind fields in our study area.

Simulations have been performed for one month (November 1999). Comparisons have been performed with wind observation in a large number of measurement locations covering the model area as well. Comparisons between the two model performances have also been presented.

Three-dimensional wind field estimates in complex terrain

1 Introduction

The results of air pollution dispersion modelling in complex terrain are entirely dependent on adequate description of the three-dimensional wind field. As part of model a verification study in a rather complex terrain the inhomogeneous and instationary winds have proven to play an important role in advecting the plumes. Several different procedures for modelling the three dimensional wind and turbulence fields have been developed and tested.

This paper presents a discussion of wind filed estimates and compare the analyses to observed winds in the area.

2 Model descriptions

Two procedures for generating the wind fields have been applied in this study. Short the descriptions of the two wind field models are presented in the following chapters.

2.1 MATHEW

MATHEW (Sherman, 1978; Slørdal, L.H., 2002) is a diagnostic wind field model able to generate a three-dimensional wind field in a Cartesian grid, based on an arbitrary number of wind observations within the model domain. The model treats variable topography within the model domain, and computes a wind field that minimizes the variances between the observations and the calculated values. In addition the computed wind field is mass conserving, e.g. a condition that is approximated in the model by requiring the flow field to be free of divergence ($\nabla \cdot \vec{V} = 0$).

2.2 TAPM

TAPM (Hurley, 2002) is a prognostic, incompressible, non-hydrostatic, primitive equation model with a terrain-following vertical coordinate for three-dimensional simulations.

The model solves the momentum equations for horizontal wind components, the incompressible continuity equation for vertical velocity, and scalar equations for potential virtual temperature and specific humidity of water vapour, cloud water and rainwater.

The model solution for winds, potential virtual temperature and specific humidity, is weakly nudged with a 24-hour e-folding time towards the synoptic-scale input values of these variables.

The Exner pressure function is split into hydrostatic and non-hydrostatic components, and a Poisson equation is solved for the non-hydrostatic component. Explicit cloud microphysical processes are included.

Solving equations for turbulence kinetic energy and eddy dissipation rate, and then using these values in representing the vertical fluxes by a gradient diffusion approach, including a counter-gradient term for heat flux, have determined the turbulence terms in these equations. A vegetative canopy and soil scheme is used at the surface, while radiative fluxes, both at the surface and at upper levels, are also included.

The model can run in a nested way, with a maximum number of 4 inner grids. The boundary conditions for the inner grids are provided from the course outer grids, by an interpolation procedure.

3 The test area and the database

3.1 Topographical features

The modelling area consists of several complex terrain features. It is bounded to the northeast by the sea, to the southwest by the 500 m high ridge running northwest-southeast, and to the east by another ridge of similar height. A rather flat valley bottom extends about 16 km from the coastline and has an average width of about 10 km. The plain is open to the north.

The temperature difference between land and sea and the nearby topographic features create local wind fields. The land-sea breeze, which is a dominant feature of the local meteorology, creates wind fields that oscillate through 180°, roughly perpendicular to coast. Locally measured winds are chiefly influenced by this feature and are only representative of the larger scale synoptic forcing when this is significantly larger than the locally induced pressure gradients. Historical data and estimates indicate that for more than 50% of the time the local wind field is de-correlated from the synoptic wind field.

Another type of local circulation may be represented by the katabatic winds during the night-time and anabatic winds during daytime that blow along sloping terrain. These effects may not be so pronounced at least in the daily convective condition, due to the relative low elevation of terrain.

In the southeast of the modelling area a channelling effect in the valley between the two ridges should be presented.

The local topography and measurement sites are shown in Figure 1 below.

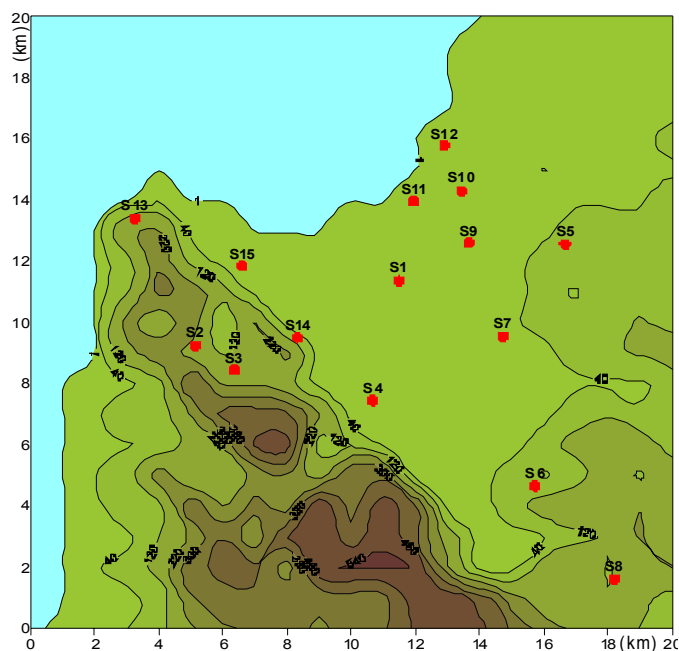


Figure 1: Modelling area showing land/sea and topography. Also included are the available meteorological sites

Due to the complex topographical features as well as the variability in surface conditions, as seen in our test area, regional meteorological models cannot reproduce the local circulations. The features of the local wind patterns will have to be estimated either by interpolation of a very dense network of local wind measurements or by local scale dynamical models. The interpolative methods can be used for diagnostic wind field estimates and used as input to diagnostic or “nowcast” models for air pollution concentration estimates.

For prognostic models it will be necessary to scale down the wind field model to predict the fields on a local scale, i.e. on a scale of typical dimensions one to five kilometre. The TAPM model enables such procedures and may be used to a certain degree for this purpose.

3.2 The measurement network and database

The test area monitoring networks as presented in Figure 1, consists of 14 air quality stations, which are also equipped with meteorological instruments for measuring wind speed, wind direction and temperature. Measurements of wind speed and wind direction at 60 m, temperature profile between 30 m and 60 m and dry and wet temperature at 2m above the surface is being measured along one 60 m high tower located in the middle of the valley. Other parameters are also measured at the tower such as turbulence parameters. These data were, however, not used in the input of the wind field analyses using the MATHEW model.

Considering the representativity of the sites, only a total number of 7 stations, including the meteorological tower data, have been considered for the analyses. These sites were S13, S8, S2, S14, S3, S5 and meteorological tower; S1.

3.3 Site representativity evaluation

A more detailed analysis that has included considerations regarding the position of the measurement points in the modelling area and their representativity related to different topographical effects has led to a reduced number of 5 representative sites for surface measurements and 2 sites where upper air winds have been generated using the dynamical weather data from the TAPM model. These selected data were considered able to reproduce an average wind field in the test area and was used for the first run of MATHEW. These 5 stations were:

- S1 – Centrally located and at 60 m is the most obvious choice.
- S5 – Representative for Easterly inland flow.
- S3 – Located at the top of the ridge.
- S13 – Representative for sea breeze effects.
- S8 – Representative for southerly flow and topographic channelling

Not all data from these 5 observation sites must be used at one run. For instance, a good representativity of the see-breeze effect could be obtained either only using S13 or S3. This statement is supported by a simple analysis of simultaneously observations at one station against another.

Figure 2 shows the scatter plots for observed wind directions from S13, S3 and S2, which are all on the ridge.

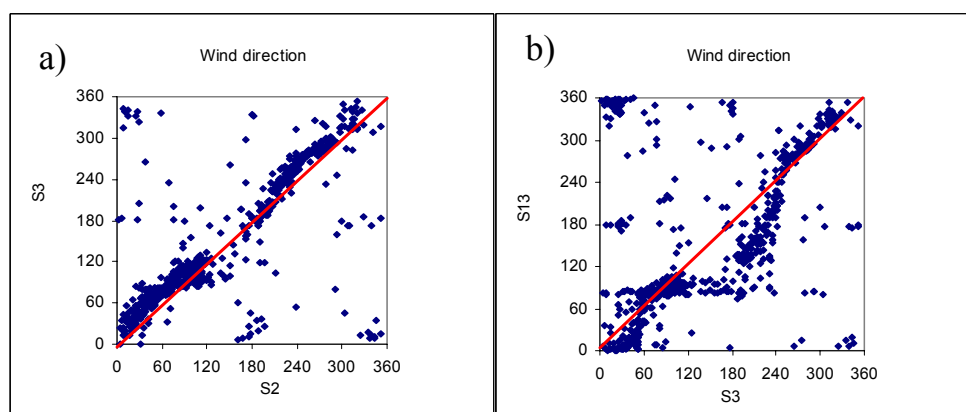


Figure 2: Scatter plots of the wind directions (degrees) at the measurement points S2, S3 and S13: a) S2 vs S3; b) S3 vs S13

The scatter plots (a) show that the measured wind direction at S2 and S3 are well correlated. As long as the observed data at both sites have a similar pattern there are reasons to assume that one of the two sites (e.g. S3) provides an adequate representation of the wind at this part of the ridge.

When analysing the scatter plots for observations at S13 and S3 (or S2) a tendency of channelling at S13 is observed when the wind blows from around east. Similarly, when the wind blows from southwest a rotation counter clockwise from S3 to S13 is observed. These are obviously local effects of channelling at S13 during land breeze conditions. Good correlations for the observed wind directions are observed during well-defined sea breezes from around northwest.

The channelling at S3 around 180-240 degrees may also be due to effects of buildings located near the station.

The reason for including the measurement point S8 was its position in the south-easterly part of the test area, where a channelling effect of the valley outflow or inland inflow wind is expected. However, the measurements at this site are undertaken in a non-open area with local obstacles influencing the microclimate at the site. Analyses of data from S8 have indicated that they may be questionable even if the instruments are quite accurate and sensitive.

4 Wind field modelled with MATHEW

For diagnostic of wind field in the test area, the MATHEW meteorological pre-processor has been run in different conditions. This makes use of point measurements for wind and temperature and, through a mass-conserving algorithm that takes into account topography, converts these points into a physically consistent wind field.

As input data MATHEW requires:

- Wind speed and wind direction at surface at least at one location
- Upper wind speed and wind direction
- Temperature gradient between two vertical levels at one location
- Topography field
- A constant roughness length over the entire modelling area was assumed.

The upper wind data are not mandatory as input. If missing upper air data, the model itself does generate (interpolate) the wind speed and wind direction from the top of the surface layer to the top of mixed layer by using different profile functions depending on atmosphere stability.

Therefore, when running such model, the first task should be the selection of the most representative measurement points that correctly reproduce the pattern of the wind field in the area. No strong local effects such as induced turbulence by buildings or other nearby obstacles should influence the measurements of wind speed and wind direction at the selected sites.

In addition to the above surface stations the MATHEW model produces more representative wind profiles when upper air data is also available. Unfortunately no such data is available in the test area, so instead model output from TAPM dynamical weather model at 400 m was used as upper air wind data in the MATHEW wind field generator.

Two different runs of MATHEW including different measurement points were performed:

- Case A: includes observed data from S1, S5, S8 and S13
- Case B: includes observed data from S1, S3 and S5

In both cases, as mentioned earlier, upper air wind data as generated by the TAPM model at S1 and S13 have been used.

The resolution of the model run was 1 km while the total grid size was 20 km x 20 km. In vertical a number of 10 layers with the following thickness 20, 30, 40, 50, 60, 100, 250, 500, 750 and 1200 m have been defined. The total model depth was thus 3000 m. The time period for the model run was one month, from 1 to 30 November 1999.

The model output is hourly, gridded values of wind speed and wind direction.

4.1 Results and comparison with observed data

The model estimates wind speed and wind direction data have been compared with the observed data at the measurement points, which were not used as input data in the model. Figure 3, Figure 4 and Figure 5 present the scatter plots of observed and modelled data for wind direction and wind speed in both runs (case A and case B specified above).

The results have been divided into site locations; in the valley, on the ridge or on the plain. The sites for comparisons with measurements were:

- S2 located on the ridge
- S4 and S15 located in the valley but close to the ridge side
- S6 located in the southeast region on a low elevated hill
- S12 located in an open plain, close to the shoreline.

4.1.1 Valley sites

The scatter plots in Figure 3 show that the model (both runs) reflects well the land and sea breeze effects. At the station S15 (case A) the interaction between slope flows and land or sea breeze effect is partially reproduced by the model based on the measured data from S13 or S3 used as model input.

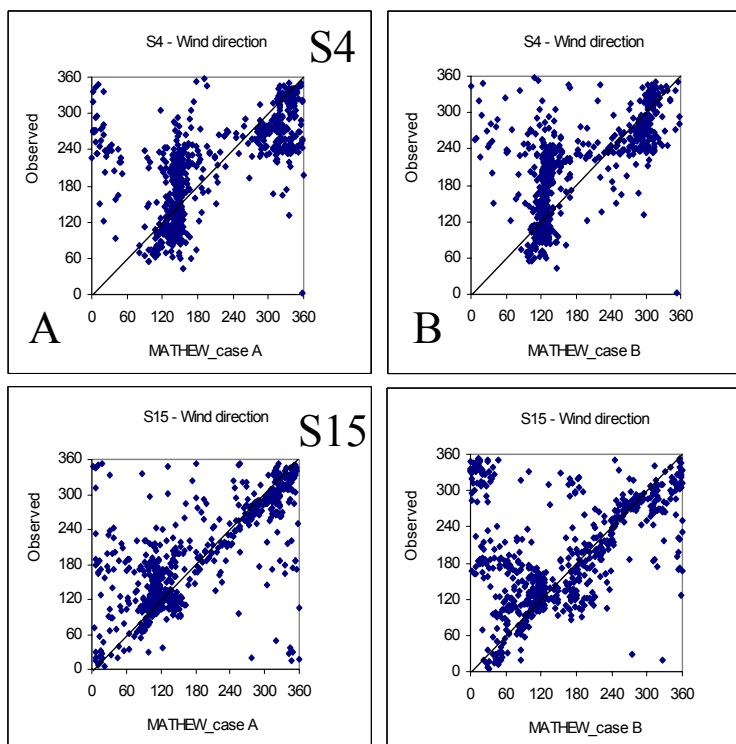


Figure 3: Scatter plots of the wind direction (degrees) modelled with MATHEW in case A, case B and the observations. The wind direction is measured at 10 m above ground, while the modelled wind direction corresponds to the middle of the first model layer (20 m thickness)

A strong channelling of south-easterly winds is generated at S4 by the model due to topographical effects along the main valley axis. However, the model cannot reproduce the local katabatic flows measured at this site during nighttime. A small valley south of the site may influence the measured wind directions to give southerly and south-westerly winds during the night.

The sea breeze during daytime hours is well reflected at both sites by the MATHEW model.

4.1.2 Ridge sites

The scatter plots in Figure 4 for the elevated site S2 indicate that the MATHEW model is reflecting the measurements well. This was expected, especially for Case B, which uses data from site S3, close to the S2. The sea breeze and land breeze is not as strongly channelled as at other sites, due to local and micro scale topographical effects. However, these effects are also reflected in the model.

At the elevated site S6 the model reflects well the land breeze as well, while the sea breeze is slightly different from the observed wind directions at the site.

However, this site is located far from the coastline and the sea breeze (from around 300 degrees) results in a large spread of observed wind directions. The observed wind seems to be influenced by local topographical effects.

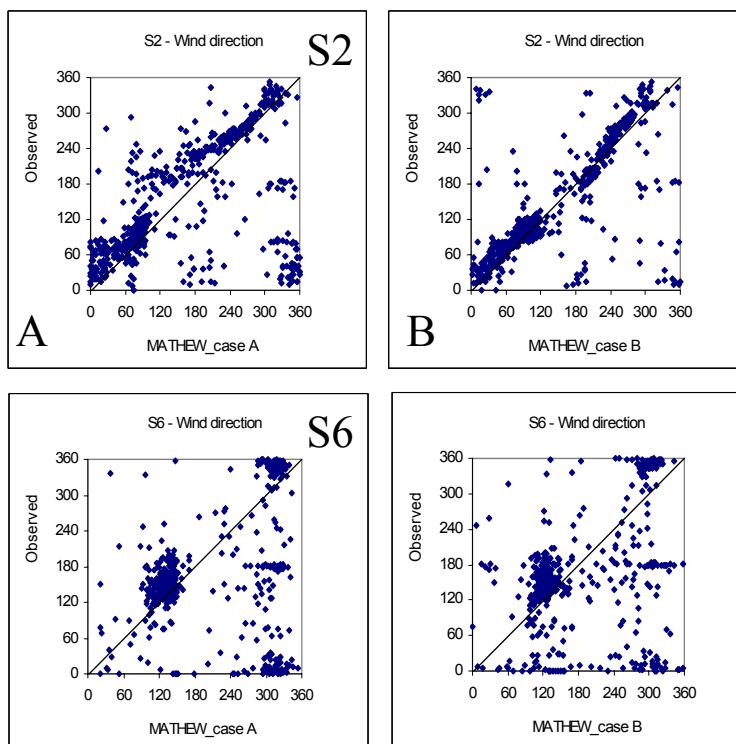


Figure 4: Scatter plots of the wind direction (degrees) modelled with MATHEW in case A, case B versus observations. The wind direction is measured at 10 m above ground, while the modelled wind direction corresponds to the middle of the first model layer (20 m thickness)

4.1.3 Open plain sites

The open plain site S11 is located very close to the shoreline. The model estimates show in both cases a fairly good agreement with the observed data and describe well both sea and land breeze effects. Small differences for onshore as well for offshore winds are still occurring. The 90 degrees observed offshore wind is turned to 120 degrees in the model, while the observed onshore winds are also slightly turned counter clockwise.

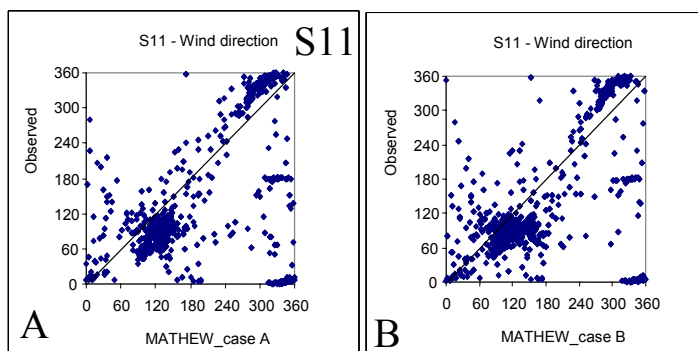


Figure 5: Scatter plots of the wind direction (degrees) modelled with MATHEW in case A, case B versus observations. The wind direction is measured at 10 m above ground, while the modelled wind direction corresponds to the middle of the first model layer (20 m thickness).

4.2 Wind speeds modelled with MATHEW

The MATHEW model reflects the observed wind speeds well at all sites. Figure 6 shows an example from site S11 located on the plain close to the coastline. Case A and B give similar results. Case B slightly overestimates the wind speeds compared to MATHEW Case A.

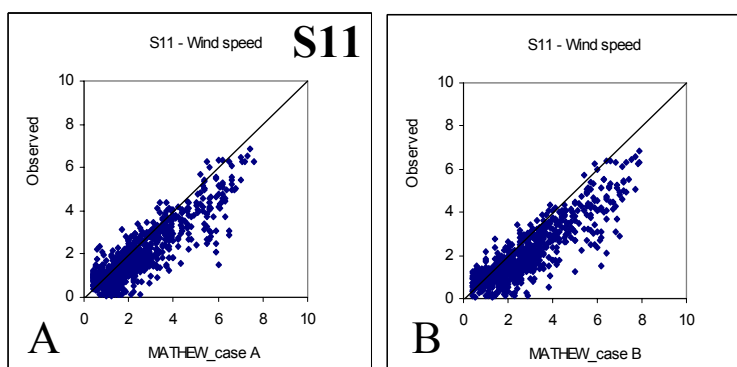


Figure 6: Observed versus estimated wind speeds using the MATHEW model at site S11.

Figure 7 shows the observed wind speeds at 2 another different sites located in the valley and on the ridge, related to model estimated wind speeds using the MATHEW model. The wind speeds were measured at 10 m above ground, while the modelled wind speed corresponds to the middle of the first model layer, which has a thickness of 20 m.

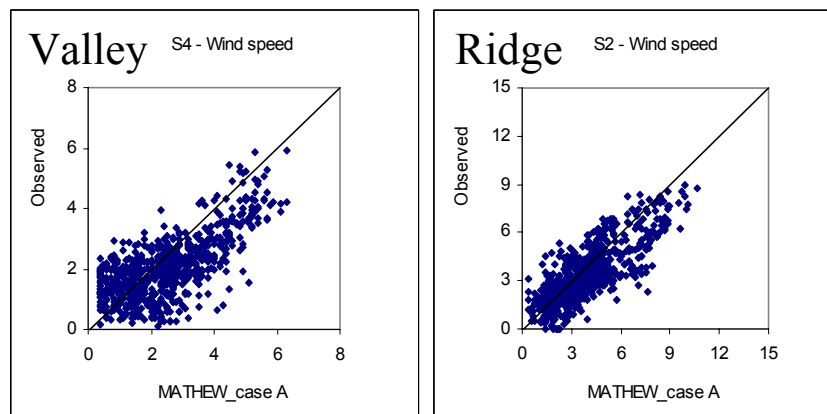


Figure 7: Observed versus model estimated wind speeds by MATHEW at different sites in the valley and on the ridge.

As an interpolation model MATHEW is strongly depending of the observed data as well as of the distribution of sites used in the model. From the figures we can see that the wind speeds on the open plain as well as at the ridge site is better reflected than in the valley.

5 Wind field modelled with TAPM

The prognostic model TAPM has been operated for the area to create meteorological data such as wind speeds, wind direction, turbulence, vertical profiles and a number of boundary layer parameters. The model does not need on-site data as the main input are based on synoptic data. As such, the meteorological data used by the model are provided by the synoptic scale analysis model (LAPS) and consists of six-hourly weather data on a longitude/latitude grid at 0,75 degree spacing (approximately 75 km).

The global terrain height data on a longitude/latitude grid at 30-second grid spacing (approximately 1 km) are based on public domain data available from the US Geological Survey, Earth Resources Observation Systems (EROS) Data Centre Distributed Active Archive Centre (EDC DAAC).

The US Geological Survey is also providing global land cover characterization data on a longitude/latitude grid at 30-second grid spaces (approximately 1 km). No soil type information was available for the study area and a default type (sandy clay loam) has been assumed for the study area.

The model has been run in the hydrostatic mode, in a three nested way starting with a 200 km x 200 km grid (20 x 20 cells, 10 km resolution), then 60 km x 60 km (3 km resolution) and finally 20 km x 20 km (1 km resolution). A number of 25 vertical layers have been defined. The total vertical model depth has been 8000 m.

The model output is complex and consists of wind field, temperature, boundary layer parameters, fluxes, turbulence field and also profile data for most of the parameters.

5.1 Results and comparison with observed data

The modelled wind speed and wind direction on the inner modelling grid have been compared with observed data at most of the measurement points. The scatter plots of modelled and observed data are presented in the following chapters.

5.1.1 Valley sites

Three sites have been selected to show the wind modelling in the valley as presented in Figure 8.

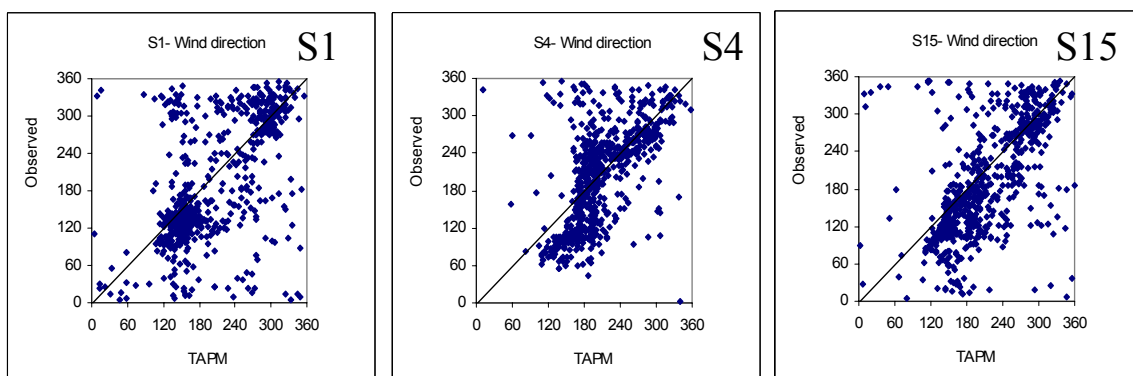


Figure 8: Scatter plots of the wind direction (degrees) modelled with TAPM at valley sites. The wind direction is measured at 10 m above ground, the modelled wind direction corresponds to the first model layer (10 m thickness) at S4 and S15 while at S1 corresponds to the 3-rd model level, (approximately 50 m above ground).

At meteorological site S1, TAPM can reflect relatively well the land breeze, while in case of sea breeze the model shows a spread of the results over a large range of wind sectors. The cases with badly corresponding wind directions are most probably due to quickly changing winds during transitional periods, which may be poorly reflected in the model.

At S4 the model produces a similar channelling as MATHEW but less pronounced. The TAPM model is able to partially reflect the interaction between land breeze and the katabatic wind that blows downhill from SSW. A better behaviour of the model occurs at S15, which is located closer to the ridge and therefore more exposed to slope winds.

5.1.2 Elevated sites

At the elevated site S2 the model seems to be more sensitive at the sea breeze effect (270 degrees) than during land breeze conditions. In the latter case the model seem to channel the wind along an axis at around 150 degrees, while the observation indicate a prevailing wind direction of around 90 degrees.

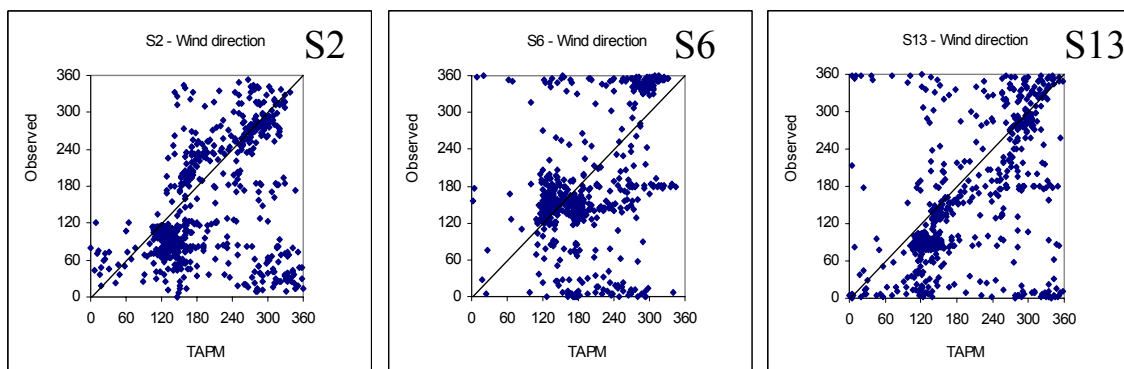


Figure 9: Scatter plots of the wind direction (degrees) modelled with TAPM at elevated sites. The wind direction is measured at 10 m above ground, while the modelled wind direction corresponds to the first model layer (10 m thickness)

At S13 the model in case of land breeze produces a similar channelling effect. Most of the land breeze cases are modelled at winds from southeast; 120-140 degrees.

The best simulation of the land breeze seems to occur at the low elevated site S6. However, for the model generated sea breezes at S6, all directions have been observed at this site. This conclusion is similar to the one stated for the MATHEW model estimates and indicates that there may be local effects modifying the observed winds at the site.

5.1.3 Open plain sites

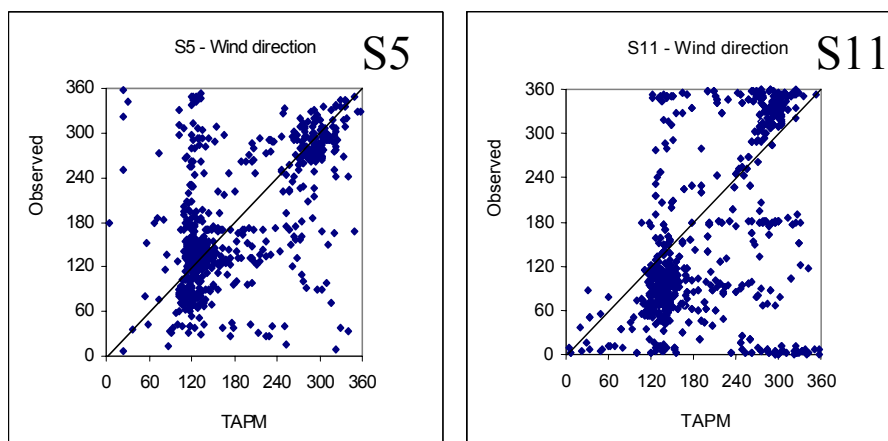


Figure 10: Scatter plots of the wind direction (degrees) modelled with TAPM at open plain sites. The wind direction is measured at 10 m above ground, while the modelled wind direction corresponds to the first model layer (10 m thickness)

At all the open plain sites (Figure 10) the TAPM model produce a well defined land breeze, which is channelled around 120 degrees. The observations during

these cases may vary from one site to another, dependent upon local influences in the observed winds.

The sea breeze at S5 is very well reflected by the TAPM model, while at S11 there is a turning in the model results to blow from NNW compared to the observed more northerly winds at S11.

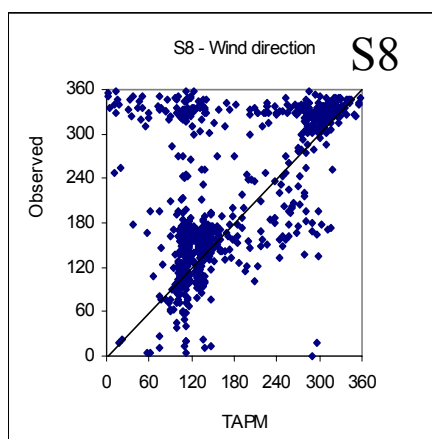


Figure 11: Scatter plots of the wind direction (degrees) modelled with TAPM at site S8.

At site S8 (see Figure 11), which is located in the south-eastern part of the model area, far from the coast line and in a flat part of the valley, the model estimated sea breezes are very different from the wind directions observed during these hours. At this location, the observed winds show a strong channelling from around 340 degrees, which is along the valley axis. The TAPM model has generated all wind directions during these hours, however, mainly from northwest and northeast. The model thus was not able to reproduce well the observed channelling effect at site 8.

5.1.4 TAPM characteristics

From the results of wind field modelling using the TAPM model it may be stated that the main differences between the model estimated winds and the observed winds seem to be related to transitions periods. This especially relates to the transitional periods from sea breeze to land breeze. However, it may also relate to the morning transition from land breeze to sea breeze. It seems that the changes in wind directions occur faster in real life observations, than the model is able to reflect.

The model for most of the sites adequately reproduces the prevailing wind directions related to land or sea breeze. At some of the measurement points local effects such as channelling by near by obstacles, are important factors in setting up the observed wind directions. It is thus not always clear whether the model simulations or the observations are more representative for the general airflow in the area.

5.2 Wind speeds modelled with TAPM

The wind speeds estimated using the TAPM model has been compared to observed wind speeds as presented in Figure 12.

As seen from the scatter plots, the TAPM model seems to overestimate the wind speed at most of the valley and open plain sites. This especially applies to winds stronger than about 6 m/s.

At the ridge site, S2, the model more often predicts stronger winds than observed, but not as strong winds as in the valley. A study of these cases has shown that the model is generating a stronger land and sea breeze than indicated in the observations.

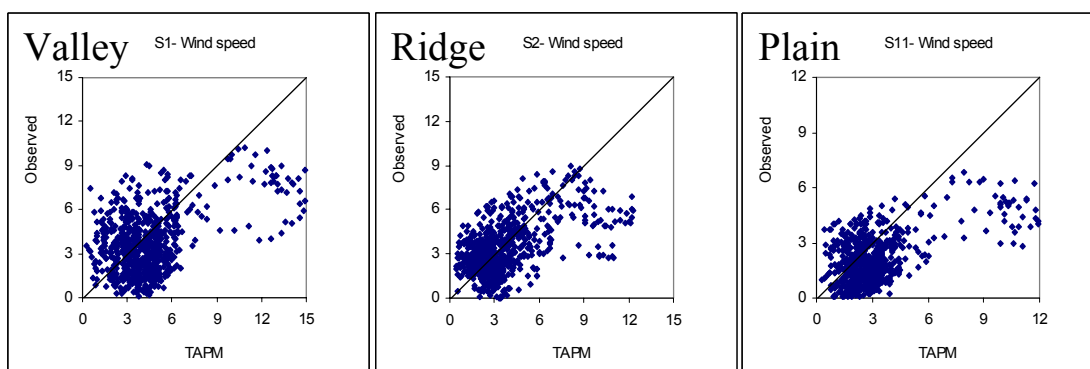


Figure 12: Scatter plots of the wind speed (m/s) modelled with TAPM. The wind speed is measured at 10 m above ground, while the modelled wind direction corresponds to the first model layer (10 m thickness).

The intensity of the marine breeze effect is proportional with the temperature gradient between sea and land. As the model considers a monthly average temperature for the sea surface, only the diurnal variation of land temperature is responsible for the temperature gradient between sea and land. Thus, the observed air temperatures at site S1 have been compared with the modelled values as presented in the Figure 13.

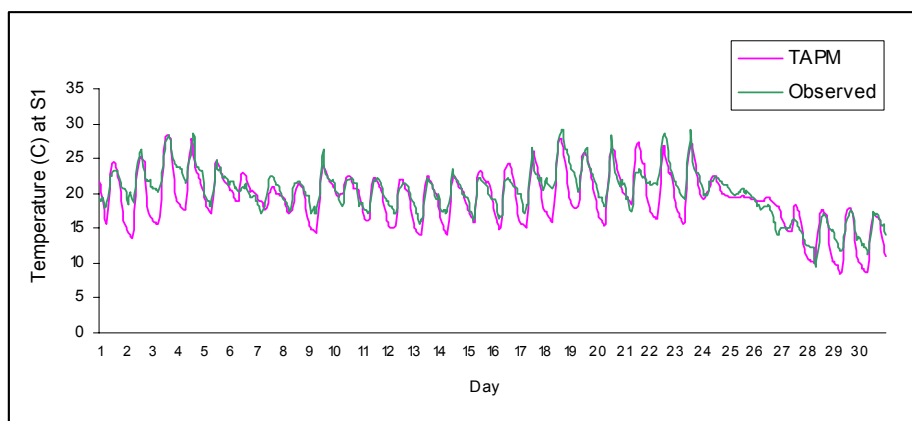


Figure 13: Comparison between modelled with TAPM and observed temperature at S1 location. The modelled temperature correspond to the 3-rd model level (50 m above ground), while the observed data correspond to 60 m above ground.

The diurnal variation of temperature is reasonable well simulated with TAPM, but as indicated in the figure, the model systematically provides an underestimation during the night time. Therefore, this can explain the stronger temperature gradient obtained with TAPM, responsible for a more intense land breeze effect during night time.

6 Comparisons of the wind field with MATHEW and TAPM

6.1.1 Wind fields

The presence of topography affects the flow in the modelling region, inducing an inhomogeneous and non-stationary wind field. Moreover, the transitional periods from sea to land breeze in the evening and from land breeze to sea breeze in the morning hours normally last between 2 to 3 hours. These transition periods often develop sudden changes in wind directions and wind speeds, which are difficult to reproduce by the models. The following simulations with MATHEW and TAPM will demonstrate the capability of models to reproduce the wind field under these various topographical conditions as well as the sensitivity of the models at the transitional periods.

The wind field obtained with MATHEW (case A and case B) and TAPM has been analysed at different hours: 0:00 (at midnight), 12:00 PM (noon), 18:00 PM (afternoon - evening).

The reason for studying the wind fields at these hours are related to the transition period from sea and land breeze as well as from anabatic to katabatic slope winds. At these hours different situations can be observed, depending on the temperature gradient between sea and land, net radiation and other parameters. The most problematic case is the transition period between land and sea breeze, when wind speeds are generally very low and there is a strong fluctuation of wind directions.

In Figure 14, which displays results for 5 November at different hours, several typical features can be seen.

1. At 00:00 hrs winds in the north-eastern part of the area are fairly consistent in all three cases. However, topographically induced flow, night time katabatic flow, visible in TAPM, is only partly present in Case B and not at all in Case A. Therefore the selection of S3 allows some of this feature to be captured.
2. At 12:00 hrs all 3 cases give similar results, with the exception of the region around S8 in Case A. The region has reverted from the offshore land breeze, seen at 00:00, to the onshore sea breeze.
3. At 18:00 hrs both Case A and B give similar results, however TAPM is at this point reverting from a sea to a land breeze state (something that in reality occurred 2 hours later) and as such shows a westerly component in the land covered region.

The above example is typical of many of the features encountered in the comparative study. The timing of the transition period, as can be seen in Figure 14, is not always well simulated by TAPM. During these periods there could also be significant difference between the two MATHEW scenarios. During the transition from land to sea breeze and visa versa, which occurs very rapidly in reality, TAPM would react more slowly to the forcing, resulting in a turning of the wind that was rarely measured at the 1 hour average time scale.

Another relevant example is depicted in the Figure 15, where, in case a) MATHEW at 12:00 hrs shows a stabilised sea breeze while TAPM is still reproducing a weak land breeze effect. In the case b) a high synoptic forcing, such as during night time on 26 November is reproduced quite well by both scenarios and TAPM (see also Figure 13, for temperature variation).

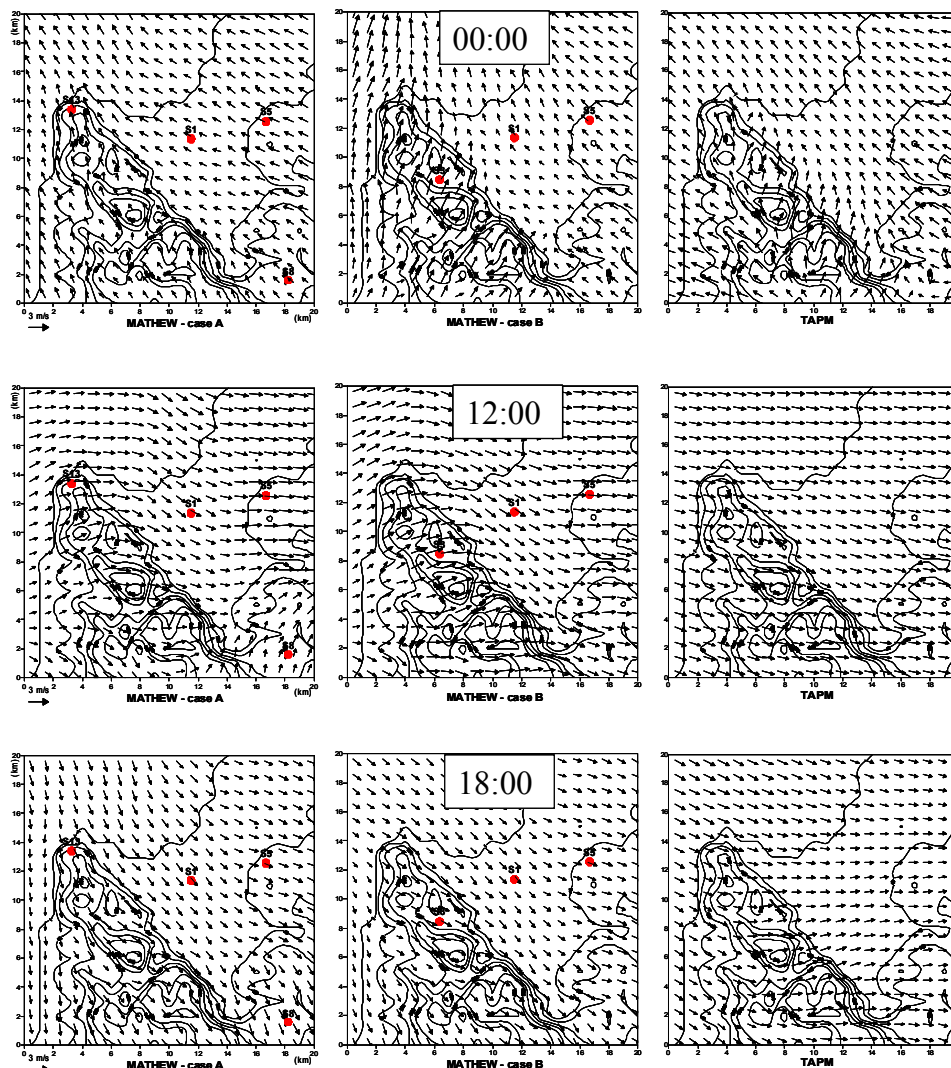


Figure 14: Wind fields produced by MATHEW for Case A (left) , Case B (centre). To the right is the wind field produced by TAPM for the same period. Top row is at 00:00, middle row at 12:00 and bottom row at 18:00. All figures are from 5 November 1999

Several conclusions can be drawn:

- S8 regularly produced inconsistent wind fields in the surrounding region when used in the Case A scenario.
- There are few differences in the resulting fields whether data from the sites S13 or S3 are being used, except in particular transition cases.
- TAPM can describe many of the physical characteristics of the wind field and often generates very similar wind fields to the MATHEW model. However, it is not always consistent, both spatially and temporally, with measurements. This is not surprising since it is forced at its boundaries, which, in the nested version in use, are roughly 100 km away.

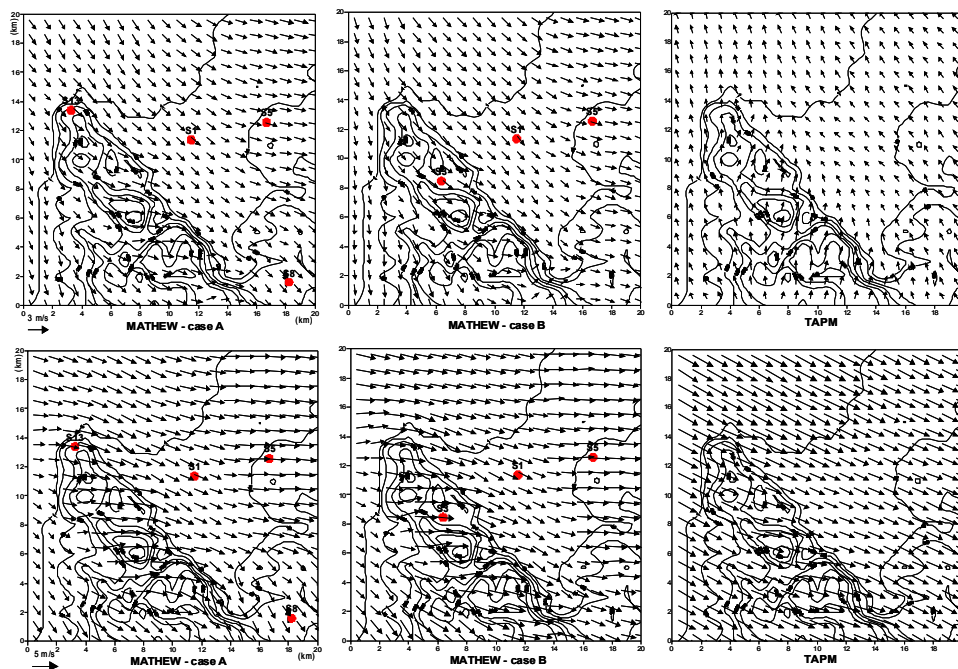


Figure 15: Wind fields produced by MATHEW for Case A (left), Case B (centre). To the right is the wind field produced by the TAPM model for the same period. Top row is at 12:00 hrs (8 November) showing a discrepancy between both models during transitional periods and bottom row at 00:00 hrs (26 November) showing a synoptic forcing during night time.

6.1.2 Wind speed profiles

When dispersion models in this area for elevated point sources are applied using a modelled wind field, the profiles of wind speed and wind direction are very important. Moreover, the complex terrain and marine breeze induce frequently winds that are strongly varying from the surface layer to upper levels. During transition periods low winds and upper winds are often completely decoupled.

Vertical wind profiles estimated using the models presented above have been compared. The main goal of these comparisons is to evaluate the differences between vertical profile output from the models as well as identifying the spatial changes in wind profiles due to complex terrain effects.

In Figure 16 a comparison of typical night time and daytime wind speeds profiles obtained with MATHEW (case A and case B) and TAPM is included. The profiles have been investigated at different locations. The sites S1, S3 and S5 coincide with the measurement point while “S top ref” is a reference point corresponding to the highest elevation of topography on the modelling area.

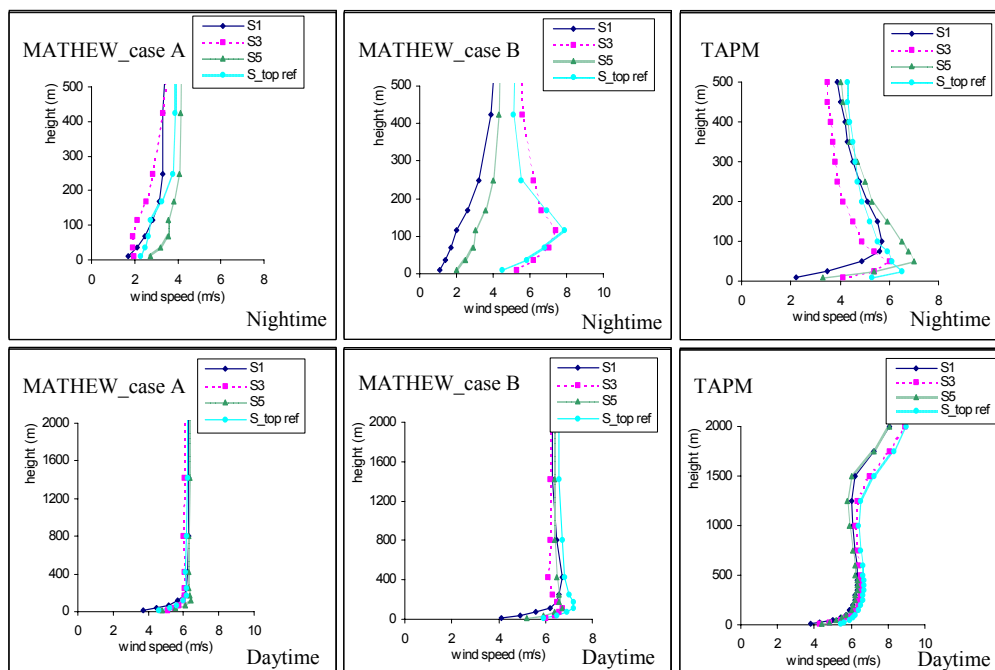


Figure 16: Typical night time (11 Nov, 4:00 AM) and daytime (11 Nov, 14:00 PM) profile data of the wind speed calculated with MATHEW in case A (left), MATHEW in case B (centre) and TAPM (right) at different locations.

During the night time MATHEW produce similar wind profiles at S1 and S5, while significant differences are occurring at ridge sites, where case B indicates a significant wind speed increase at around 100 m above the surface. The TAPM model predicts higher winds at the surface both at the valley sites and on the plain compared to the results of the MATHEW model. This is the case even compared to the MATHEW case B results for the ridge sites.

6.1.3 Wind direction profiles

The profile of wind directions Figure 17 show also differences at elevated sites for MATHEW runs. TAPM indicates similar profiles to case B at ridge sites but a discrepancy at S1 consisting of a significant wind shear over the first 100 m is observed.

However, both models predict similar wind directions between 120 and 180 degrees corresponding to the regularly direction of offshore land breeze in the modelling area.

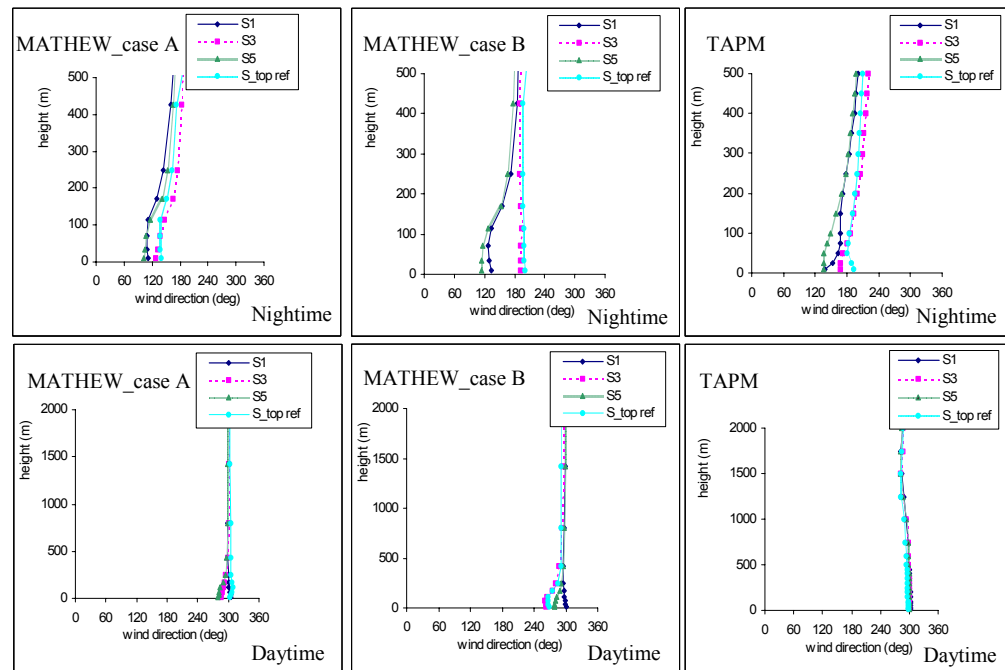


Figure 17: Typical night time (11 Nov, 4:00 AM) and daytime (11 Nov, 14:00 PM) profile data of the wind direction calculated with MATHEW in case A (left), MATHEW in case B (centre) and TAPM (right) at different locations

During daytime both models produce more horizontally homogeneous profiles in wind speeds and wind directions. TAPM predicts a constant wind speed and direction over the entire modelling area indicating a strong and dominant sea breeze effect. The wind direction estimated with MATHEW slightly oscillates from 240 to 300 degrees from one site to another.

As a conclusion, the wind profiles seem to be quite well simulated during daytime, while during night time they are different and in case of MATHEW strongly depends of the positions of involved observation points. Over topography the flow generally dominated by stronger wind speed with high gradients close to surface is better simulated with MATHEW in case B than in case A, due to observed data from S3 that are used as input in the model.

7 Conclusions

Both models predict quite well the wind field in the modelling area, showing similar pattern in many cases. Differences are mainly encountered during transition period from the onshore sea breeze to off shore land breeze and vice versa. Especially the TAPM model is not sensitive enough to reflect the sudden changes in wind directions observed at most sites. The TAPM model seems to have an inertia that cannot represent these sudden changes. The MATHEW model seem to reflect these cases better.

The MATHEW model also generates reasonable results as long as the observed data used in model interpolation estimates are representative and not influenced

by local and micro scale effects at the measurement sites. This can be seen when using data from measurement point S8 for case A estimates. This case has produced some doubtful results.

The TAPM model is able to predict a wind field that incorporates the physics of many processes that actually occur in the modelling area. The complete set of equations for wind, temperature and humidity field, together with the radiative scheme, cloud microphysics and boundary layer parameterisation has been demonstrated able to describe the horizontal in-homogeneities in temperature fields induced by the influence of complex terrain. The effects of sea breezes and land breezes as well as any other effects that are generated by the horizontal radiative forcing have been well simulated by the model.

8 References

- Hurley, P. (2002) The Air Pollution Model (TAPM) Version 2, Part 1: technical description (CSIRO Atmospheric Research Technical Paper No.55).
URL: http://www.dar.csiro.au/publications/hurley_2002a.pdf.
- Hurley, P., Physick, W. and Luhar, A. K. (2002) The Air Pollution Model (TAPM) Version 2, Part 2: summary of some verification studies (CSIRO Atmospheric Research Technical Paper No.57).
URL: http://www.dar.csiro.au/publications/hurley_2002b.pdf.
- Physick, W., Hurley, P., Blockley, A., Rayner, K. and Mountford, P. (2002) Verification of the air quality models TAPM and DISPMOD in coastal regions. In: *Proceedings of the 4th International Conference on Environmental Problems in Coastal Regions, Rhodes, Greece, 16-18 September 2002*, pp. 16-18.
- Sherman, C.A. (1978) A mass consistent model for wind fields over complex terrain. *J. Appl. Meteorol.*, 17, 312-319.
- Shir, C.C. (1973) A preliminary numerical study of atmospheric turbulent flows in the idealized planetary boundary layer. *J. Atmos. Sci.*, 30, 1327-1339.
- Slørdal, L.H. (2001) Bruk av MATHEW i AirQUIS/Episode 03. Revisjon av eksportrutine. Kjeller (NILU TR 03/2001).
- Slørdal, L.H. (2002) MATHEW as applied in the AirQUIS System. Model description. Kjeller (NILU TR 09/2002).
- Slørdal, L.H., Walker, S.E. and Solberg, S. (2003) The urban air dispersion model EPISODE. Technical description. Kjeller (NILU TR in prep.).

